Transport of weak-electrolyte anions through anion exchange membranes: Current-voltage characteristics

4 AUTHORS, INCLUDING:

Natalia Dmitrievna Pismenskaya
Kuban State University
60 PUBLICATIONS   1,011 CITATIONS

SEE PROFILE

Victor Nikonenko
Kuban State University
93 PUBLICATIONS   1,768 CITATIONS

SEE PROFILE

Gerald Pourcelly
Université de Montpellier
169 PUBLICATIONS   3,089 CITATIONS

SEE PROFILE

Transport of weak-electrolyte anions through anion exchange membranes
Current–voltage characteristics

Natalia Pismenskaya [a], Victor Nikonenko [a], Bernard Auclair [b], Gérald Pourcelly [c,*]

[a] *Department of Physical Chemistry, University of Kuban, Krasnodar, Kuban, Russia*
[b] *Laboratoire des Matériaux Echangeurs d'Ions, Université Paris XII, Paris, France*
[c] *Institute Européen des Membranes, Université Montpellier II, IEM-UMR 5635, CC047, 34095 Montpellier Cedex 5, France*

Abstract

Transport of salts of phosphoric and carbonic acids through anion exchange membranes (AEM) is studied by means of current–voltage responses. Concentration polarisation of such membrane systems is accompanied by a change in the electrolyte concentration at the membrane–solution interface due to hydrolysis reactions. Current–voltage characteristics (CVC) on HPO_4^{2-} or PO_4^{3-} ion-containing systems with modified AEM selectively permeable to mono-charged anions present two waves like in electrode multi-component systems with multi-stage electrochemical reactions. This phenomenon does not occur with nonmodified AEMs. It is also the case with all the AEMs studied for solutions containing HCO_3^- or CO_3^{2-} salts because of close values of electrical resistances of the membranes in these both ionic forms. © 2001 Elsevier Science B.V. All rights reserved.

1. Introduction

In regions with intensive farming, natural waters generally contain a great amount of hydrocarbonate-, carbonate-ions and products of dissolution of phosphate fertilisers, which may exist in a form of dihydrophosphate-, hydrophosphate- and phosphate-ions. Electrodialysis methods are the most available ones to remove these ions to improve the quality of water. Despite the actual necessity of studying transport mechanisms of weak-electrolyte anions through ion exchange membranes, there are several works only

dealing with this problem [1–4]. It is basically connected with experimental and theoretical difficulties caused by hydrolysis, i.e. interaction of salt ions with water that leads to the formation of a weak-electrolyte [5]. Concentration polarisation of membrane systems is accompanied by a change in the electrolyte concentration [6] and the solution temperature [7,8] at the membrane/solution interface. Besides, under currents close to the limiting one and exceeding it, water splitting accelerated by catalytic active ionogeneous groups of the ion exchange membranes takes place at the interfaces [9–13]. These factors change the hydrolysis degree [5] complicating the interpretation of the data obtained. Consequently, the knowledge of peculiarities of the membrane transport in carbonate and phosphate-containing solutions is of great

* Corresponding author. Tel.: + 33-467-149110;
fax: +33-467-149119.
E-mail address: pourcell@iemm.univ-montp2.fr (G. Pourcelly).

importance for the choice of ion exchange materials and optimisation of conditions for the electrodialysis process. The present work therefore deals with the study of transport characteristics of AFN, AMX, ACS, ACM anion exchange membranes in contact with solutions containing HCO_3^-, CO_3^{2-}, $H_2PO_4^-$, HPO_4^{2-}, PO_4^{3-} as well as SO_4^{2-} ions, the latter are also found in natural waters but take no part in hydrolysis reaction.

2. Experimental

The AFN, AMX, ACS and ACM membranes are produced by Tokuyama Soda [14]. The main characteristics of the anion exchange membranes (AEMs) studied are collected in Table 1. The values are that of the suppliers, checked at the Laboratory of Membrane and Materials Processes in Montpellier.
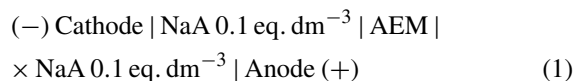
The specific weight of the AEMs was determined by measuring both their dimensions and weights after a 3-day drying of the membrane samples in the chloride form at 45°C.

The data on the electrical conductivity of the AFN, AMX, ACS and ACM membranes in HCO_3^-, CO_3^{2-}, $H_2PO_4^-$, HPO_4^{2-}, PO_4^{3-} and SO_4^{2-} ion forms, that have already been published in [15], were completed by the data on the electrical conductivity in the OH^- ion form using the clip-cell described in [16].

Current–voltage curves (CVC) were obtained in galvanodynamic mode using a classical two compartment no-flow cell described in [17]. This measurement cell was composed of two symmetrical 100 cm³ half-cells (the wide part of the cell). These compartments are separated by two Viton@ gaskets, which clamp the membrane. In the geometrical center of the gaskets, there was a cylindrical hole (the narrow

part of the cell). The working area of the AEM was 0.5 cm². Two Ag/AgCl electrodes immersed into Luggin capillaries allowed the measurement of the potential difference between two equipotential planes near the two membrane–solution interfaces. Mechanical stirrers were placed in each compartment. The electrical current was supplied with two platinum coated titanium electrodes. The electrical circuit was composed of a Tacussel PRT-40-1XT potentiostatic generator monitored by a PIL-101T signal generator.
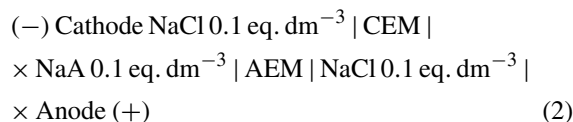
The cell configuration was

$$(-)\, \text{Cathode} \mid \text{NaA } 0.1\, \text{eq. dm}^{-3} \mid \text{AEM} \mid$$
$$\times \text{NaA } 0.1\, \text{eq. dm}^{-3} \mid \text{Anode } (+) \qquad (1)$$

where 'A' is the anion.

The rate of the current scanning was 0.01 mA/s.

To determine pH variations occurring with the current increase during CVC measurements, distinct experiments were made for membranes AFN, ASC in phosphate and dihydrophosphate ion forms. In this case, the cell configuration was

$$(-)\, \text{Cathode NaCl } 0.1\, \text{eq. dm}^{-3} \mid \text{CEM} \mid$$
$$\times \text{NaA } 0.1\, \text{eq. dm}^{-3} \mid \text{AEM} \mid \text{NaCl } 0.1\, \text{eq. dm}^{-3} \mid$$
$$\times \text{Anode } (+) \qquad (2)$$

(CEM is the auxiliary cation exchange membrane), where the previous CVC cell (1) was completed with a third compartment. This three-compartment configuration with reversible Ag/AgCl electrodes prevented any variation of pH due to electrode reactions. The pH of the depleted and enriched solutions was measured in the vicinity of membrane interfaces with the help of pH-meter WTW pH 320 and pH-combined electrode SenTix50. The measurements were made at a steady-state of the system. Currents were specified from a smaller value to a higher one. Before each

Table 1
Main characteristics of the AEMs studied (from suppliers)[a]

	AFN	AMX	ACS	ACM
EC meq./g Cl-form of dry membrane	2.0–3.5	1.4–1.7	1.4–2.0	1.4–1.7
WC gH$_2$O/g Cl-form of dry membrane	0.40–0.55	0.25–0.30	0.20–0.30	0.13–0.18
ER $\Omega\,cm^2$ in 0.5 eq. dm^{-3} NaCl	0.4–1.5	2.5–3.5	2.0–2.5	4.0–5.0
Thickness (μm)	150–200	160–180	150–200	110–130
Specifications	Resistant against organic fouling	High chemical strength	Mono-anion permselective	Low proton transport

[a] AFN, AMX, ACS, ACM from Tokuyama Soda are homogeneous and contain quaternary ammonium groups [14].

application of the current, the solutions in the half-cells were renewed.

All the measurements were carried out at $25 \pm 0.5°C$.

3. Results

3.1. Electrical conductivity

The data on the electrical conductivity of AEMs in NaOH solutions are presented in Fig. 1. They are reported along with other values of the electrical conductivity data obtained earlier [15,18] (Table 2). The data show that the values of the electrical conductivity of the AFN, AMX, ACS membranes in the OH$^-$ ion form are much higher than those in any salt

Table 2
Electrical conductivity of AEMs in contact with different 0.05 eq. dm^{-3} solutions (mS cm^{-1})[a]

	AFN	AMX	ACS	ACM
NaOH	17.8	8.9	3.0	0.027
NaCl[b]	8.3	4.3	2.5	1.0
NaNO$_3$[b]	17	2.6	1.8	0.5
NaF[a]	15.5	4.8	2.0	1.0
Na$_2$SO$_4$[c]	12.8	2.8	0.58	0.20
NaHCO$_3$[c]	11.8	2.8	0.56	0.22
Na$_2$CO$_3$[c]	12.4	3.5	0.52	0.24
NaH$_2$PO$_4$[c]	4.2	1.0	0.21	0.06
Na$_2$HPO$_4$[c]	9.4	2.1	0.18	0.08
Na$_3$PO$_4$[c]	9.4	1.7	0.13	0.02

[a] Errors on determination: $\pm 5\%$.
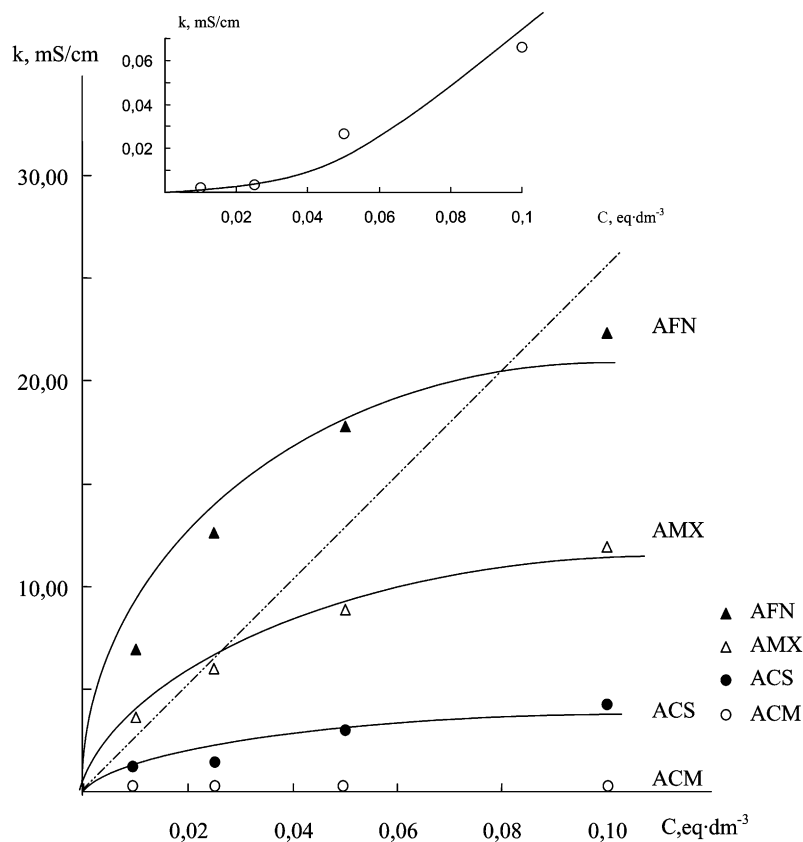[b] From [18].
[c] From [15].

Fig. 1. Concentration dependence of electrical conductivity of AEMs in contact with NaOH solutions. The straight line is the conductivity of the solution. Intercepts are isoconductivity points. (Zoom: conductivity of the ACM membrane).
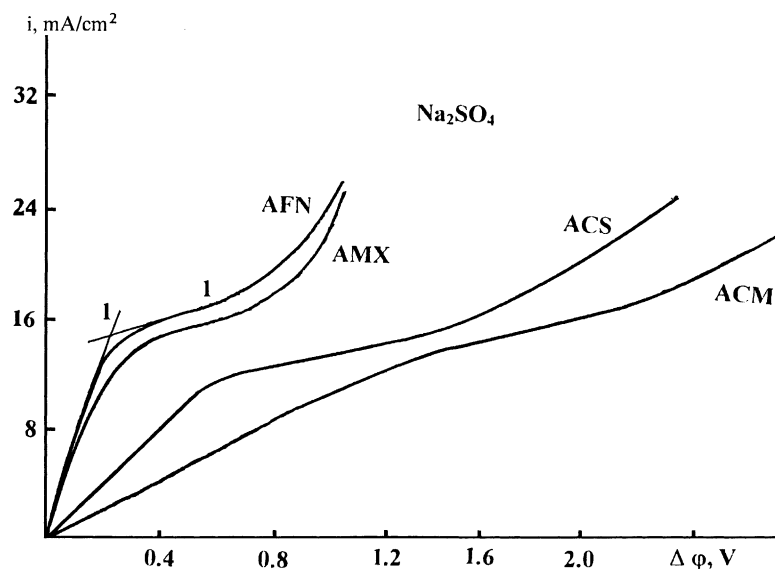
Fig. 2. CVC for different AEMs in contact with $0.1\,\mathrm{eq.\,dm^{-3}}$ solution of Na_2SO_4.

anion form. For the ACM membrane, the electrical conductivity value in OH^- ion form is closed to that in PO_4^{3-} form, which has the lowest value of conductivity among the anionic forms studied. The electrical conductivity of the membranes in the OH^- form as well as in the salt anion forms studied [15,18] grows according to the sequence

$$ACM < ACS < AMX < AFN \qquad (3)$$

3.2. Current–voltage curves (CVC)

CVC of anion exchange membranes AFN, AMX, ACS and ACM, equilibrated with $0.1\,\mathrm{eq.\,dm^{-3}}$ solutions of Na_2SO_4, $NaHCO_3$, Na_2CO_3, NaH_2PO_4, Na_2HPO_4, Na_3PO_4 are shown on Figs. 2–7.

In hydrocarbonate and carbonate (Figs. 3 and 4) solutions, the shape of the CVC is similar to the curves obtained for Na_2SO_4 solutions (Fig. 2). For these
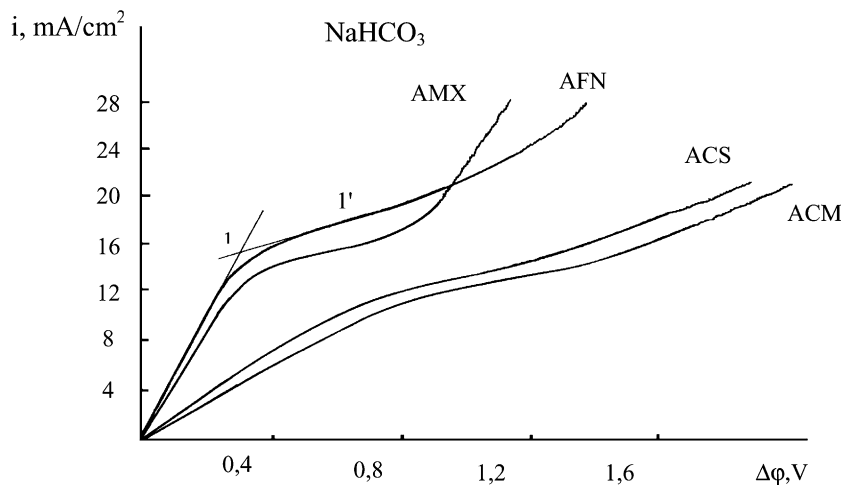
Fig. 3. CVC for different AEMs in contact with $0.1\,\mathrm{eq.\,dm^{-3}}$ solution of $NaHCO_3$.
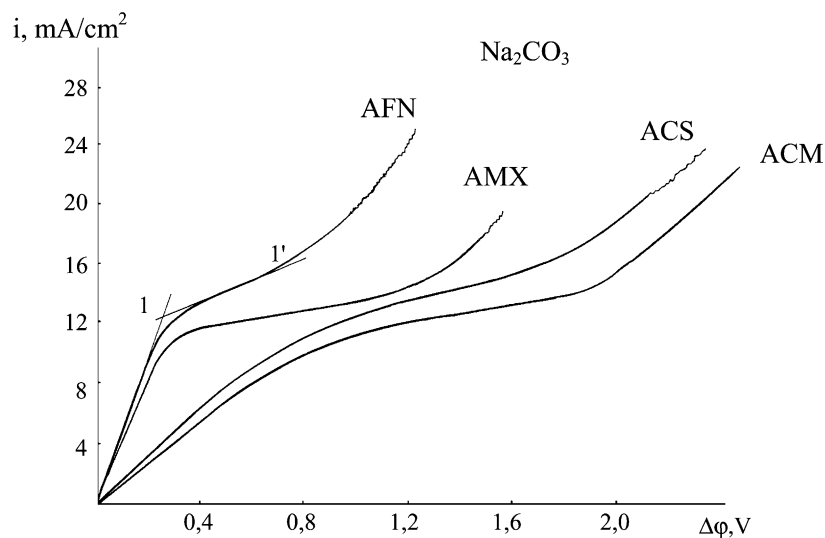
Fig. 4. CVC for different AEMs in contact with 0.1 eq. dm^{-3} solution of Na$_2$CO$_3$.

systems, the CVC have one horizontal plateau and one limiting current determined by the cross-point of the tangents drawn from two neighbouring plate parts of the curve (point 1 in Fig. 2). The CVC shape for phosphate, hydrophosphate and dihydrophosphate systems differs from the traditional one (Figs. 5–7). In sodium phosphate solutions (Fig. 5), the CVC shape for the

AFN and AMX membranes is close to an usual one. For the ASC and ACM membranes with a modified surface, there are two plateaus (between points 1 and 1′ as well as 2 and 2′, where 1′ and 2′ are the inflection points of the CVC). The CVC for the membranes equilibrated with the sodium hydrophosphate solution (Fig. 6) are close to sodium phosphate ones, though
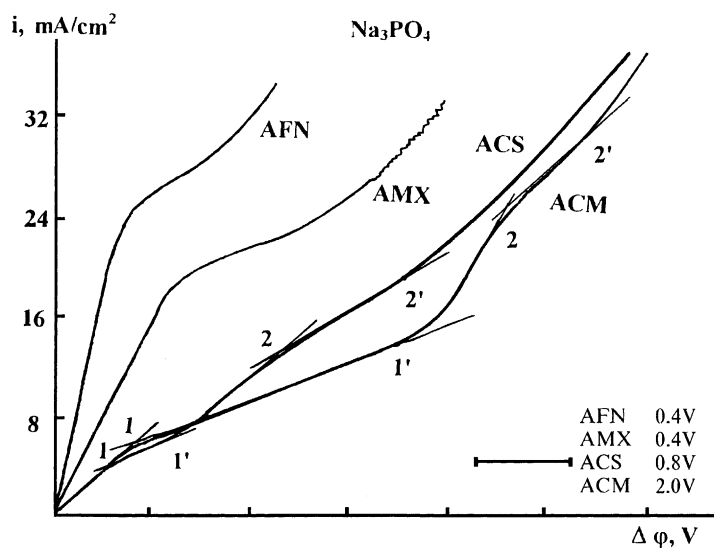

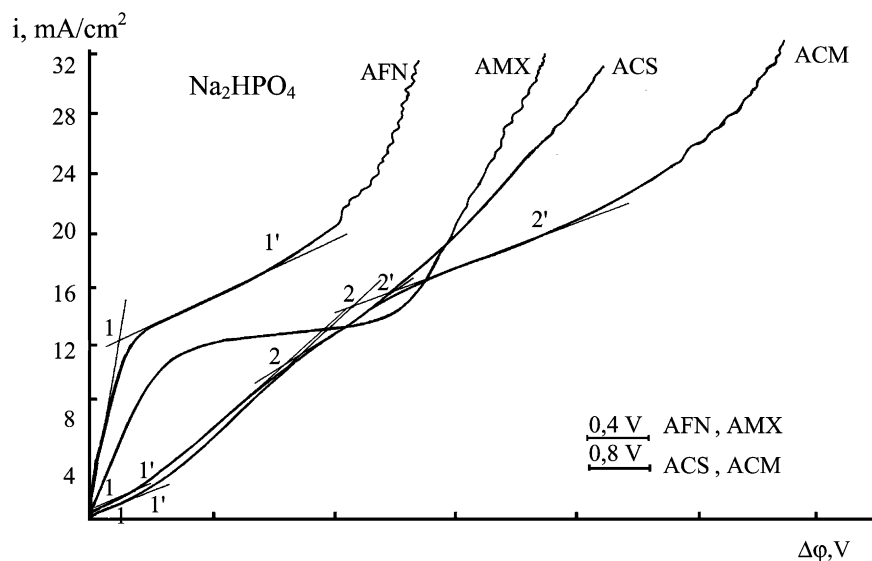Fig. 5. CVC for different AEMs in contact with 0.1 eq. dm^{-3} solution of Na$_3$PO$_4$.

Fig. 6. CVC for different AEMs in contact with $0.1\,eq.\,dm^{-3}$ solution of Na_2HPO_4.

plateau $1-1'$ on these curves is less developed than in the Na_3PO_4 solution (Fig. 5). In the NaH_2PO_4 solution, two plateaus and two limiting currents $i_{cr.1}$ and $i_{cr.2}$ (points 1 and 2 on the CVC) are observed for all membranes studied (Fig. 7).

Note, that the values of the potential drops for ACS and ACM membranes (especially for ACM) at points 2 and $2'$ of CVC are very high (Figs. 5–7). For instance, the values of these potential drops for the ACM membrane in the PO_4^{3-} ion form are equal to 8.5 and
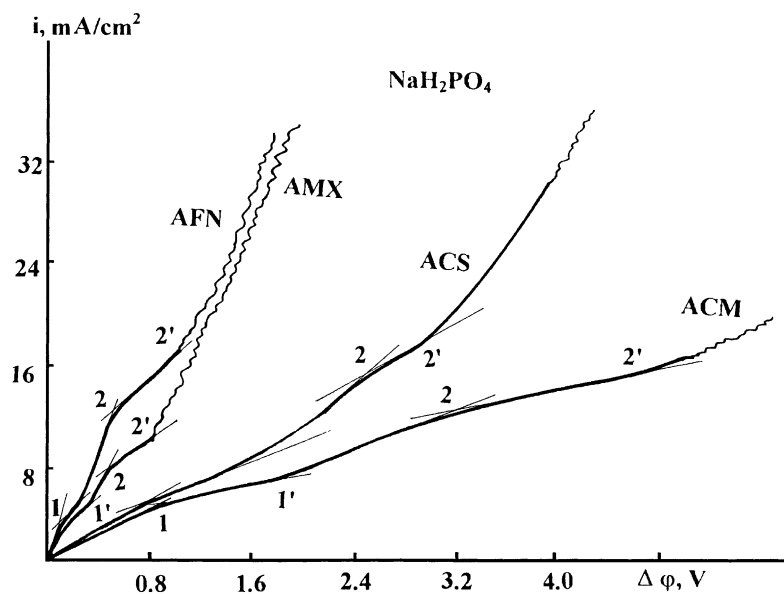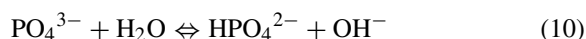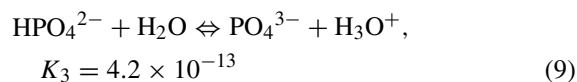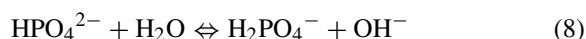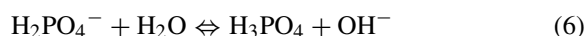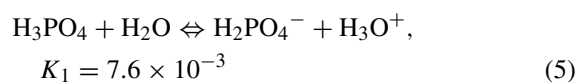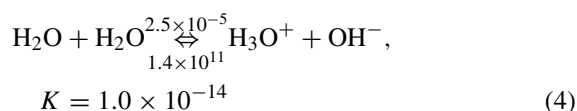

Fig. 7. CVC for different AEMs in contact with $0.1\,eq.\,dm^{-3}$ solution of NaH_2PO_4.

12.0 V, respectively, evidently due to relatively high electrical resistance of this membrane (Table 2).

4. Discussion

Before starting the discussion, let us note that the studied membranes differ in cross-linked degree, ion exchange capacity, porosity and water content (Table 1), but the nature of the membranes is similar. All of them are homogeneous and contain quaternary ammonium bases $N(CH_3)_3^+$ as ionogeneous groups. Perhaps, ACS and ACM membranes have a surface modification that makes the membranes selective to mono-charged anions.

In contrast with salts of strong acids (NaCl, NaF, $NaNO_3$, Na_2SO_4), salts of weak-acids take part in the hydrolysis reaction. In phosphate aqueous solutions, the following chemical reactions resulting in alkali (6, 8, 10) or acid formation (5, 7, 9) take place [19]

$$H_2O + H_2O \overset{2.5\times10^{-5}}{\underset{1.4\times10^{11}}{\Leftrightarrow}} H_3O^+ + OH^-,$$
$$K = 1.0 \times 10^{-14} \tag{4}$$

$$H_3PO_4 + H_2O \Leftrightarrow H_2PO_4^- + H_3O^+,$$
$$K_1 = 7.6 \times 10^{-3} \tag{5}$$

$$H_2PO_4^- + H_2O \Leftrightarrow H_3PO_4 + OH^- \tag{6}$$

$$H_2PO_4^- + H_2O \Leftrightarrow HPO_4^{2-} + H_3O^+,$$
$$K_2 = 6.2 \times 10^{-8} \tag{7}$$

$$HPO_4^{2-} + H_2O \Leftrightarrow H_2PO_4^- + OH^- \tag{8}$$

$$HPO_4^{2-} + H_2O \Leftrightarrow PO_4^{3-} + H_3O^+,$$
$$K_3 = 4.2 \times 10^{-13} \tag{9}$$

$$PO_4^{3-} + H_2O \Leftrightarrow HPO_4^{2-} + OH^- \tag{10}$$
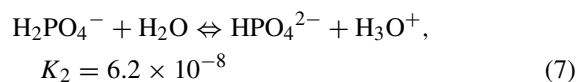
Above and under the arrows are the rate constants of direct reaction κ_1' and reverse reaction κ_{-1}'. The constants of equilibrium K are given after reactions. In accordance with the chemical equilibrium constants,
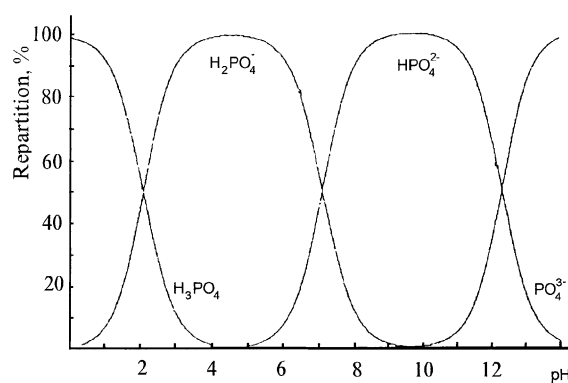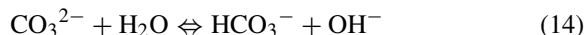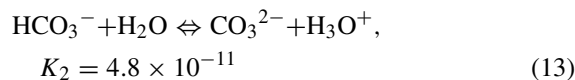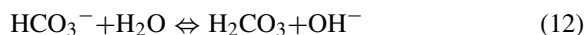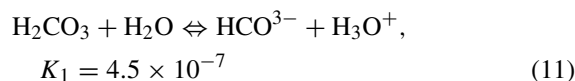

Fig. 8. Diagram of repartition of phosphorous-containing species vs. pH (from [15]).

the solution is alkaline for phosphate and hydrophosphate solutions as presented in the diagram of phosphate species partition (Fig. 8). Dihydrophosphate solutions are acidic.

In hydrocarbonate and carbonate solutions, the following reactions may occur [20]:

$$H_2CO_3 + H_2O \Leftrightarrow HCO^{3-} + H_3O^+,$$
$$K_1 = 4.5 \times 10^{-7} \tag{11}$$

$$HCO_3^- + H_2O \Leftrightarrow H_2CO_3 + OH^- \tag{12}$$

$$HCO_3^- + H_2O \Leftrightarrow CO_3^{2-} + H_3O^+,$$
$$K_2 = 4.8 \times 10^{-11} \tag{13}$$

$$CO_3^{2-} + H_2O \Leftrightarrow HCO_3^- + OH^- \tag{14}$$

As shown in Fig. 8, the amount of $H_2PO_4^-$ and HPO_4^{2-} ions is maximum (close to 100%) for pH values equal to 4.4 and 9.4, respectively. When pH is equal to 2.0 or smaller, only H_3PO_4 species remains in the solution. When pH is over 13, only PO_4^{3-} ions are in the solution.

The solution contains the maximum amount of HCO_3^- and CO_3^{2-} (close to 100%) for the pH values equal to 8.4 and 12.6, respectively. When the pH value is lower or close to 4.0, the solution contains H_2CO_3 (Fig. 9) only. It is alkaline in the CO_3^{2-} form and acid in the H_2CO_3 one.

As the hydrolysis reaction is a reversible process, a pH variation changes the proportion of different ion forms in the solution [5].
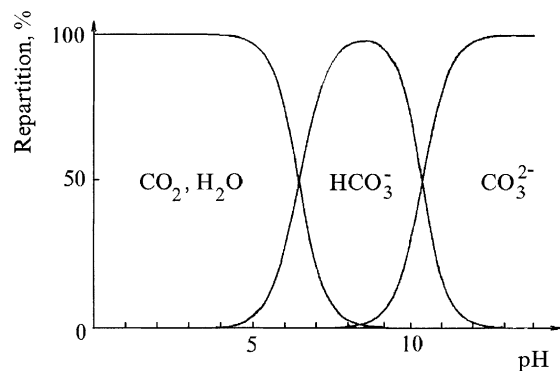
Fig. 9. Diagram of repartition of carbon-containing species vs. pH (from [16]).

4.1. Electrical conductivity of the membranes

Comparison of the electrical conductivity of the membranes in a salt anion and hydroxyl forms (Table 2) allows us to conclude that OH^- ions have the highest mobility in AFN, AMX, ACS membranes. This result correlates with the literature data, according to which the conductivity of the membranes with quaternary ammonium bases in OH^- form considerably exceeds this value for all other anion forms. For example, the conductivity of the MA-41 Russian commercial membrane, containing the same ionogeneous groups as the membranes studied is 2.3, 1.6 and 1.3 times higher in the hydroxyl form than in hydrocarbonate, carbonate and chloride forms, respectively [21]. Probably, the low value of the ACM membrane conductivity in the OH^- form is due to special properties of the modified surface layer of the membrane. The low permeability of the ACM membrane in regard to OH^- ions leads to its high electrical resistance in alkali phosphate solutions (pH = 13.5) under direct current (Fig. 5). The sequence (3) of the membrane electrical conductivity under alternating current (Table 2) is in a good qualitative agreement with the slope of the CVC curves under sufficiently low voltage (Figs. 2–7), which characterizes their conductivity under direct current.

4.2. Anomalous current–voltage characteristics

Concerning the analysis of the CVC, let us consider firstly the phosphorous-containing membrane systems (Figs. 5–7). In most cases, the shape of these CVC seems to be similar to the CVC of the electrode systems characterised by multi-stage electrochemical reactions with several limiting currents [22].

In the membrane systems containing $PO_4{}^{3-}$ ions (Fig. 5), the concentration of OH^- ions in solutions is comparable with that of $PO_4{}^{3-}$ ions (pH $\approx$ 13.5 according to Fig. 8). The mobility of OH^- ions in solutions is the highest among all the anions. Besides, as it was discussed above, the mobility of these ions in a membrane with quaternary ammonium bases considerably exceeds this value for all other anions. At small voltages, OH^- ions are therefore primarily removed from the depleted diffusion layer. As a result, the pH of the depleted solution adjacent to the membrane decreases in comparison with the pH in the bulk, and the pH of the enriched layer increases (Fig. 8). Fig. 10a shows that the pH of the depleted layer diminishes almost linearly from 12 to 3 (the case of AFN membrane) or 4 (the case of ASC membrane). So, as it follows from Fig. 8, the main charge carriers in this layer are $HPO_4{}^{2-}$ ions at low voltages and $H_2PO_4{}^-$ ions at high voltages. At sufficiently intensive currents (approximately equal to the limiting current), there is a drastic decrease of the pH of the depleted layer, that leads to a more intensive H^+ ions generation. At the limiting current, the interfacial concentrations of all salt ions become small compared to their bulk concentrations, that causes more active participation of H^+ ions in the current transfer in the depleted layer. The pH value in the enriched layer is about 10–12 (Fig. 10a), therefore the current is mainly transported by $HPO_4{}^{2-}$ ions. As it was discussed in our previous paper [15], the concentration of OH^- ions inside a membrane equilibrated with a dilute solution is always larger than in the external solution due to Donnan exclusion of H^+ ions. This phenomenon causes dissociation of $HPO_4{}^{2-}$ and $H_2PO_4{}^-$ ions entering the membrane from the diluted solution. The H^+ ions generated in this reaction returns to the dilute solution making it more acidic, $PO_4{}^{3-}$ (and $HPO_4{}^{2-}$) ions pass through the membrane and capture H^+ ions in the enriched solution making it more basic. The fact that the pH growth in the enriched layer is greater in the case of the AFN membrane is explained also by the selectivity of the ACS membrane for mono-charged anions. The transport of the multi-charged anions $HPO_4{}^{2-}$ and $PO_4{}^{3-}$ through the AFN membrane
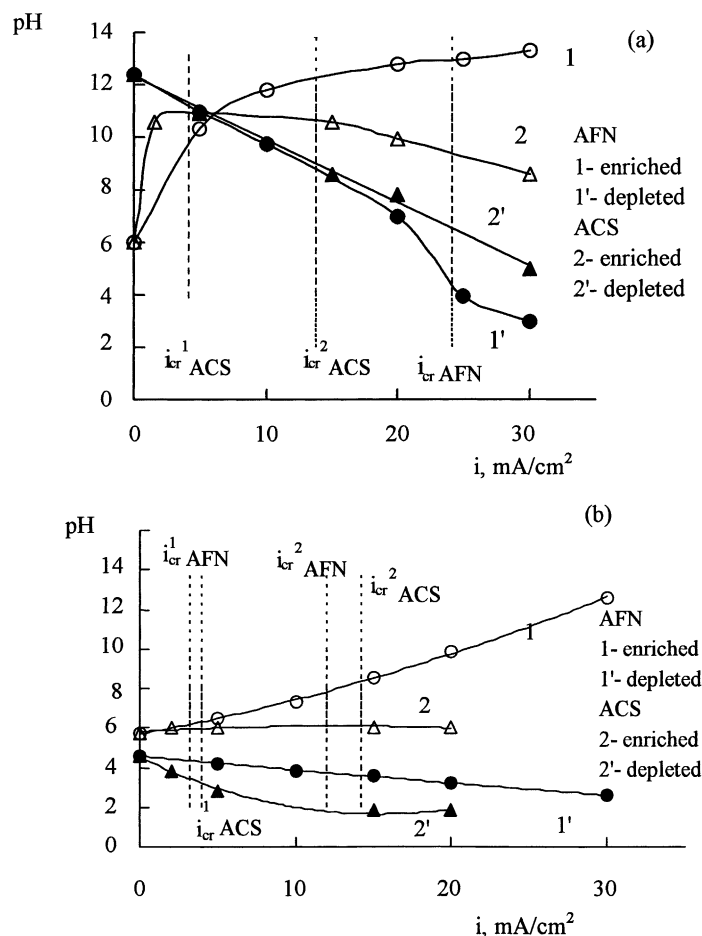
Fig. 10. Dependence of the pH value in the enriched (curves 1, 2) and depleted solution layers (curves $1'$, $2'$) near AFN (curves 1, $1'$) and ACS (curves 2, $2'$) membranes in contact with 0.1 eq. dm^{-3} solutions of Na$_3$PO$_4$ (a) and NaH$_2$PO$_4$ (b). Dotted lines are the values of the critical current densities in points 1 and 2 of the CVC. The data are obtained in the membrane system ($-$|NaA|AEM|NaCl|$+$), where A is PO$_4$$^{3-}$ or H$_2$PO$_4$$^-$ ion.

is greater then through the ACS membrane under similar conditions; the interaction of HPO$_4$$^{2-}$ and PO$_4$$^{3-}$ ions with water leads to an increase in pH value.

In AFN and AMX membranes systems, no peculiarities on CVC are observed (Fig. 5). These membranes are selective to mono-charged anions, therefore the resistance of the membranes does not vary significantly during the current growth, when the nature of the charge carrier changes. The CVC of the ACS and ACM membrane systems have two waves. The possible explanation is the following. The first wave

is due to removal of OH$^-$ ions from the depleted layer (these ions pass selectively through the modified layer of these membranes, as it was discussed). The change of the carrier for multi-charged PO$_4$$^{3-}$ (or HPO$_4$$^{2-}$) ions causes the membrane resistance increase and the first plateau (between 1 and $1'$ points) is observed. The following decrease of the pH in the depleted layer (Fig. 10a) causes a next change of the current carrier for mono-charged H$_2$PO$_4$$^-$ ions, for which the membrane is well permeable; this change raises the current–voltage curve between points $1'$ and 2. In the vicinity of point 2 (the inflection point)

the interfacial concentrations of all salt ions become so small that the fluxes of these ions reach their limiting values. The contribution of H^+ and OH^- ions in current transfer under these conditions becomes more and more important, and it causes the last rise of the CVC.

Apparently, the mechanism of the mass transfer in hydrophosphate membrane systems is similar to that in phosphate one: the removing of OH^- ions from the diffusion depleted layer leads to acidification of this layer and transformation of HPO_4^{2-} into $H_2PO_4^-$ ions. The concentration of OH^- ions in hydrophosphate solutions is lower than in phosphate one, therefore the value of current at point 1 is smaller too. The plateau 1–1′ on the CVC corresponding to the current transfer by multi-charged ions is shorter in the case of the ASC and ACM membranes in Na_2HPO_4 solution (Fig. 6) than in the Na_3PO_4 system (Fig. 5).

In the systems with NaH_2PO_4 solution we observe two plateaus on the CVC for all membranes studied (Fig. 7). Apparently, dissociation of $H_2PO_4^-$ ions inside the membranes leads to the formation of H^+ and HPO_4^{2-} ions. With increasing of the current applied, the quantity of H^+ ions, transferred from the membrane into the depleted layer, grows (that is observed in experiment, Fig. 10b) and leads to the formation of weakly dissociated form of H_3PO_4. One can imagine two mechanisms explaining two plateaus on CVC. The first considers the changes in the depleted solution layer. The depletion of the diffusion layer in $H_2PO_4^-$ ions is accompanied by accumulating H_3PO_4 in this layer. When the most part of $H_2PO_4^-$ ions is removed from the depleted layer, the current carrier species concentration gets small and a new dissociation of H_3PO_4 becomes possible, that could give the second rise to the CVC. The second explanation deals with the conductivity of the membrane phase. When the $H_2PO_4^-$ ions are removed from the depleted layer, and H_3O^+ ion concentration increases, the pH value in the membrane internal solution should decrease too. In result, the equivalent fraction of $H_2PO_4^-$ ions in the membrane should increase in comparison with multi-charged forms (mainly with HPO_4^{2-} form). As the membrane conductivity in $H_2PO_4^-$ form is less than in HPO_4^{2-} form (at least for AFN and AMX membranes, Table 2) the resistance of the membrane system grows that gives an inclined plateau (between points 1 and 1′). As Table 2 shows the

conductivity of membranes studied in HCO_3^- and CO_3^{2-} forms are close. Therefore, only one plateau on CVC in $NaHCO_3$ solutions could be observed, following the second hypothesis; that is in accordance with Fig. 3.

When the pH value gets sufficiently small (pH = 2.5), H_3O^+ ions contribution in the current becomes noticeable and the conductivity of the depleted layer increases again. Probably, the active generation of H_3O^+ and OH^- ions that is due to water splitting on ionogeneous groups of the membranes occurs at high currents (near and to the right from point 2′). Indeed, a sharp rise of the pH of the AFN membrane's enriched layer is observed at these currents.

The CVC of hydrogen–carbonate and carbonate solutions (Figs. 3 and 4) differ from phosphorous containing systems in that only one limiting current was observed. In accordance with the equilibrium constants, one may expect that appearance of the nondissociated form (H_2CO_3) in the depleted layer occur at higher pH values than in phosphorous containing systems. Therefore, the concentration of H_2CO_3 may be noticeable at very small currents and does not change dramatically with the current growth to give a critical point on the CVC like point 1 on CVC for the dihydrophosphate systems (Fig. 7). At the same time, the degree of H_2CO_3 dissociation increases with the solution diluting. Hence, in diluted solutions one can expect that the behaviour of the hydrocarbonate systems to be similar to the dihydrophosphate one. Indeed, when studying the electrodialysis process of a dilute solution containing 1.5 meq. dm^{-3} of each: hydrocarbonate, chloride, nitrate and sulphate of potassium, two plateaus on the CVC are observed for desalination channels formed by the MK-40 and MA-41 membranes [23]. Note also that the conductivity of MA-41 in the HCO_3^- form is significantly less than in the CO_3^{2-} form [21] that explains the two plateaus according to the second hypothesis.

One can see that the behaviour of membrane systems with weak-acid anions is sufficiently complicated. The fact that the dissociation is a slow process for several acids may play an important role in the interpretation of the experimental results. For a better understanding of the transport of weak-acid anions through ion exchange membranes, a mathematical modelling of the phenomena would be useful.

5. Conclusions

Anion exchange systems with weak-acid sodium salts exhibit different behaviour when studying current–voltage characteristics. In several cases, the CVC has two waves like in the electrode multi-component systems with multi-stage electrochemical reactions. This behaviour is manifested by PO_4^{3-} ion-containing systems with surface modified membranes ACS and ACM: two waves are explained by the fact that these membranes are selectively permeable to mono-charged anions. After removing OH^- ions from the depleted diffusion layer, the main current carrier becomes multi-charged anions for which the membrane resistance is high. When the pH in the depleted layer becomes sufficiently low, the mono-charged anions transfer the current and the membrane resistance decreases.

In $H_2PO_4^-$ ion-containing solutions, all the membranes show two waves on the CVC. Two hypothesis are discussed to explain this behaviour: one considers changes in the depleted diffusion layer resistance with a current growth, and the other changes in the membrane resistance.

In carbon-containing systems only one wave CVC is observed. Probably, this is connected with the fact that the difference in resistance of the membranes studied in HCO_3^- and CO_3^{2-} forms is small, and the rate of H_3O^+ ions generation is not sufficient for necessary mutual transformations of HCO_3^- ion and H_2CO_3 molecules.

Acknowledgements

References

[1] A. Lounis, C. Gavach, Electrotransport of carbonate and hydrogen carbonate ions in anion exchange membranes, J. Membr. Sci. 54 (1990) 63–74.

[2] O.A. Vysotskaia, L.A. Melnik, B.J. Kornilovich, Influence of ion-exchange bed on removing degree of boron at electro-dialysis desalination, Khimiya i Tekhnologiya wody (USSR), J. Chem. Technol. Water 20 (1988) 408–413.

[3] N.V. Eliseeva, V.V. Shaposhnik, Peculiarities of carbonate-ions transfer through anion exchange membrane at electro-dialysis, Electrokhim. Rus. J. Electrochem. 36 (2000) 1022–1025.

[4] R.P. Alison, The continuous electrodeionization process, American Desalination Association 1996 biennial conference and exposition, Monterey, CA, USA, 4–8 August 1996.

[5] B.V. Nekrasov, Bases of Chemistry, Khimiya (Chemistry), Moscow, 1973, p. 391.

[6] F. Helferich, Ionenaustauscher Grundlagen Struktur — Herstelling Theory, Verlag, GMBH, Weinheim Bergstr., 1959, p. 490.

[7] M.V. Pevnitskaya, Mass-transport enhancement in the electrodialysis of dilute solutions, Electrokhimiya 28 (1992) 1708–1715.

[8] M.V. Pevnitskaya, Mass-transport enhancement in the electrodialysis of dilute solutions, Russ. J. Electrochem. 28 (1992) 1690–1696.

[9] R. Simons, The origin and elimination of water splitting during water demineralisation by electodialysis, Desalination 28 (1978) 41–42.

[10] V.I. Zabolotsky, N. V Sheldeshov, N.P. Gnusin, Dissociation of water molecules in systems with ion-exchange membranes, Uspekhi Khimii 57 (1988) 1047–1114.

[11] V.I. Zabolotsky, N. V Sheldeshov, N.P. Gnusin, Dissociation of water molecules in systems with ion-exchange membranes, Russ. Chem. Rev. 57 (1988) 801–808.

[12] N.D. Pismenskaya, Electrodialysis of dilute solutions: the influence of pH on the transport of salt ions, Electrokhimiya 32 (1996) 277–284.

[13] N.D. Pismenskaya, Electrodialysis of dilute solutions: the influence of pH on the transport of salt ions, Russ. J. Electrochem. 32 (1996) 252–258.

[14] NEOSEPTA, Ion-Exchange Membranes, Catalogue, Toku-yama Soda Co. Ltd.

[15] N. Pismenskaya, V. Nikonenko, A.E. Allattar, G. Pourcelly, B. Auclair, E. Laktionov, Dependence of composition of anion-exchange membranes and their electrical conductivity on concentration of sodium salts of carbonic and phosphoric acids, J. Membr. Sci. 181 (2001) 185–197.

[16] Membranes polymères échangeuses d'ions, Caractérisation et méthodes d'essais des membranes homopolaires, Norme Française NF X 45-200, AFNOR, 1995.

[17] Ph. Sistat, G. Pourcelly, Chronopotentiometric response of an ion-exchange membrane in the under limiting current range: transport phenomena within the diffusion layers, J. Membr. Sci. 123 (1997) 121–131.

[18] A. Ellatar, A. Elmidaoui, N. Pismenskaia, C. Gavach, G. Pourcelly, Comparison of transport properties of monovalent anions through anion-exchange membranes, J. Membr. Sci. 143 (1998) 249–261.

[19] H. Roques, Fondements Théoriques du Traitement Chimique des Eaux, Technique et Documentation, Vol. II, Lavoisier, 1990, pp. 523–904.

[20] H. Roques, Fondaments théoriques du traitement chimique des eaux, Technique et Documentation, Vol. I, Lavoisier, 1990, pp. 1–522.

[21] V.I. Zabolotsky, N.P. Gnusin, A.I. Meshechkov, G.A. Dvorkina, Active resistance of membranes to alternating current with account of inhomogeneity of the membranes, Elektrokhimiya (Electrochemistry) 21 (1985) 1044–1048.

[22] L.I. Antropov, Theoretical Electrochemistry, Vysshaya shkola, Moscow, 1975, p. 568.

[23] K. Kesore, C. Janovski, V.A. Shaposhnik, Highly effective electrodialysis for selective elimination of nitrates from drinking water, J. Membr. Sci. 127 (1997) 17–24.